

Study of local carbon transport on graphite, tungsten and molybdenum test limiters in TEXTOR by $^{13}\text{CH}_4$ tracer injection

A. Kreter^{a,*}, P. Wienhold^a, D. Borodin^a, S. Brezinsek^a, S. Droste^a, T. Hirai^b, A. Kirschner^a, A. Litnovsky^a, V. Philipps^a, A. Pospieszczyk^a, U. Samm^a, O. Schmitz^a, G. Sergienko^a, TEXTOR Team^a

^a Institut für Plasmaphysik, Forschungszentrum Jülich, Association EURATOM-FZJ, Trilateral Euregio Cluster, 52425 Jülich, Germany¹

^b Institut für Werkstoffe und Verfahren der Energietechnik, Forschungszentrum Jülich, Association EURATOM-FZJ, Germany²

Abstract

$^{13}\text{CH}_4$ was injected through an aperture in a roof-like test limiter covered by a graphite, tungsten or molybdenum plate during Ohmic discharges. The evolution of the deposition pattern was studied by *in situ* reflectometry during each plasma pulse. Amounts of locally deposited ^{13}C and co-deposited background ^{12}C in each shot were determined *post-mortem*. The ^{13}C deposition efficiency is in a range of 0.05–0.2% and grows with the increasing amount of ^{12}C . For the same ^{12}C content the efficiency is of 0.11% for tungsten, 0.14% for molybdenum and 0.17% for graphite.

© 2007 Elsevier B.V. All rights reserved.

PACS: 52.40.Hf; 52.55.Fa; 82.80.Ch; 82.80.Ms

Keywords: Amorphous films; Carbon-based materials; Erosion and deposition; First wall; High-Z material; Molybdenum; Sputtering; Surface analysis; TEXTOR; Tracer materials; Tungsten

1. Introduction

Tungsten and carbon fiber composite (CFC) are candidate materials for plasma-facing components (PFCs) of the ITER divertor [1]. It is important to clarify to what extent eroded carbon will be trans-

ported along the carbon surfaces and to the neighbouring tungsten PFCs and deposited there. The overall balance of co-deposited tritium will depend on the carbon deposition efficiencies for different PFC materials.

$^{13}\text{CH}_4$ tracer injection is a powerful tool to investigate the local carbon transport. Well-defined amounts of $^{13}\text{CH}_4$ are injected through an aperture in a test limiter into an active discharge. *Post-mortem* analysis can distinguish between injected ^{13}C and ^{12}C from the background plasma, hence the

* Corresponding author. Fax: +49 2461612660.

E-mail address: a.kreter@fz-juelich.de (A. Kreter).

¹ www.fz-juelich.de/ipp.

² www.fz-juelich.de/iwv.

^{13}C deposition efficiency (the number of locally deposited ^{13}C atoms divided by the number of injected ^{13}C atoms) can be determined. In TEXTOR, a number of $^{13}\text{CH}_4$ injection experiments with a roof-like aluminium limiter [2] as well as spherically shaped tungsten and graphite [3] test limiters were performed in the past. For spherical limiters a large difference in ^{13}C deposition efficiency of 0.3% for tungsten and 4% for graphite was observed. Experiments presented here were performed to investigate the influence of the substrate material on the local ^{13}C transport in a roof-like geometry with a constant magnetic field inclination angle. Tungsten (W) and fine-grain EK98 graphite (C for carbon) represent the ITER divertor material choice. Molybdenum (Mo) was also selected as it is situated around the mid-point between C and W on the atomic mass scale. Mo and W are also of particular interest as they are candidate materials for diagnostic mirrors in ITER [4].

2. Experiment and results

A roof-like graphite block was covered, in turn, by 2 mm thick plane plates of polished tungsten, molybdenum and graphite inclined at 20° with respect to the magnetic field. The limiters were positioned by means of a lock system in the scrape-off layer (SOL) of TEXTOR [5] with their tips at the last closed flux surface (LCFS) at a minor plasma radius of 0.46 m. The injection channel with a diameter of 1.7 mm ended 15 mm behind LCFS. The geometry of the test limiter was similar to that used in the previous experiment with a roof-like limiter and can be found in [2]. Operating capabilities and spectroscopic observation geometry of the limiter

lock system are described in [6]. The limiters were exposed in successive Ohmic discharges at a toroidal magnetic field of $B_t = 2.25$ T and a plasma current of $I_p = 350$ kA with a central line-integrated electron density of $\bar{n}_{e0} = 2.5 \times 10^{19} \text{ m}^{-3}$ and a typical duration of 5.5 s. About $(7\text{--}8) \times 10^{19}$ $^{13}\text{CH}_4$ molecules were injected from 1 s to 4 s in the flat-top phase of each discharge. Fig. 1 shows a photograph of the tungsten plate after its exposure with the amorphous layer of co-deposited carbon and hydrogen/deuterium (a-C:H) near the injection aperture. Interference in the semi-transparent a-C:H layer produces colour fringes according to the film thickness (Fig. 2). The layers have an elongated shape in the direction corresponding to the SOL plasma flow parallel to the magnetic field combined with the $E \times B$ force, as indicated in Fig. 1.

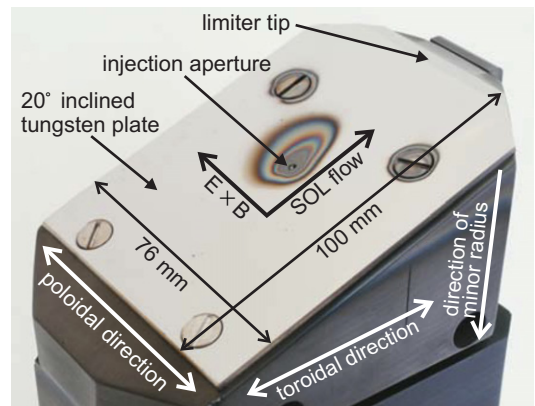


Fig. 1. Photograph of the limiter block covered by the tungsten plate after the exposure. Toroidal and poloidal directions as well as directions of the minor radius, the SOL plasma flow and the $E \times B$ force are indicated.

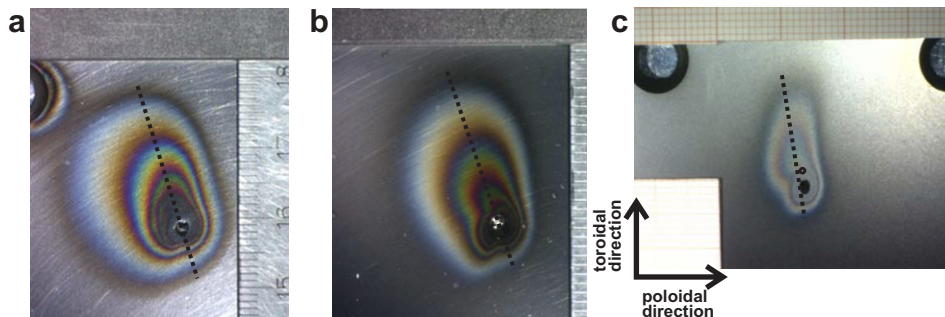


Fig. 2. Photographs of the a-C:H layers deposited near the injection aperture on (a) tungsten, (b) molybdenum and (c) graphite plates. Toroidal and poloidal directions are indicated. The colour fringe structure was used for colorimetry. Dotted lines indicate the directions of the profile scans in Fig. 3. The circle near the injection aperture of the graphite plate is the position of the SIMS depth profile in Fig. 4.

Independent of ^{13}C , a ^{12}C dominated background deposition was deposited on the target surface. This layer has a shape of a stripe across the limiter in poloidal direction and was most pronounced on the graphite plate with a maximum of $\sim 10^{18} \text{ C/cm}^2$ for a radial position 2 cm outside LCFS. On the molybdenum plate the amount of deposited carbon was at the detection limit of colorimetry of $\sim 10^{17} \text{ C/cm}^2$, on tungsten it fell below the detection limit.

The plates were observed from the top by the spectroscopic system equipped with a H_α interference filter. Observing the appearance and movement of the H_α interference fringes near the injection aperture we obtained the amount of deposited carbon *in situ* for both high- Z limiters, whereas the reflectivity from the graphite surface was insufficient for the quantification. This analysis method is often referred to as reflectometry. The result shows a continuous build-up of the layer from shot to shot (Fig. 3(a) and (b)). Reflectometry observations also indicate the net-erosion of the layer in the phase of the discharge when the $^{13}\text{CH}_4$ injection was deactivated.

The area covered after the first injection increased only little in the subsequent shots. Each new layer grew on the top of the old one increasing primarily the thickness of the film. This result is in agreement with the previous experiment in the roof-like geometry [2], whereas for the spherical limiters the contribution of the increasing area to the total layer volume was more prominent than the increase in thickness [3].

After their exposure the plates were analysed *ex situ*. By means of the colorimetry technique the colour patterns of the films (Fig. 2) were transformed into their thickness distributions. Fig. 3 shows thickness profiles of all three plates in the direction of the maximal layer elongation. Comparison of the colorimetry profiles for W and Mo limiters with those from reflectometry after the last discharge gives fair agreement, even though reflectometry delivers thickness values for the profile wing closest to LCFS lower by 20–30% as compared to colorimetry.

Sputter depth profiling by secondary ion mass spectrometry (SIMS) was applied to obtain the distributions of ^{12}C and ^{13}C . Fig. 4 shows an example of a depth profile at a position close to the injection aperture on the graphite limiter. The stratification of the layer allows us to separate the ^{13}C fractions of total carbon amount shot by shot. Combining

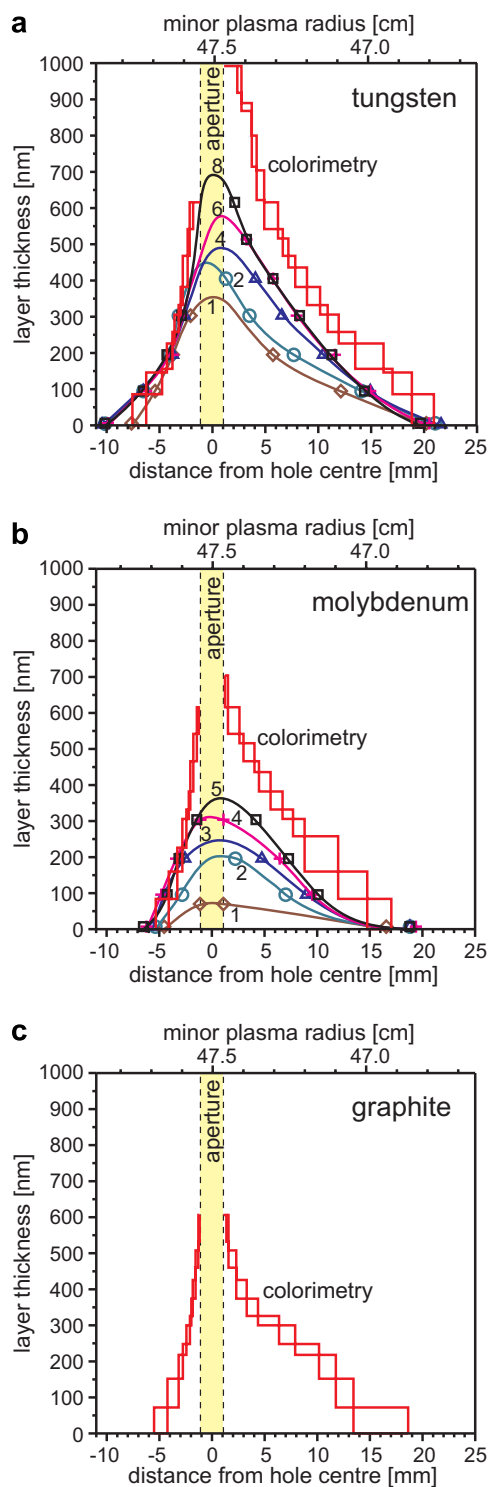


Fig. 3. Layer thickness profiles for (a) tungsten, (b) molybdenum and (c) graphite along the directions indicated in Fig. 2. Symbols connected by curves are the reflectometry data for the labelled exposure number. Colorimetry data are shown as chains of boxes each representing the position of a certain colour fringe.

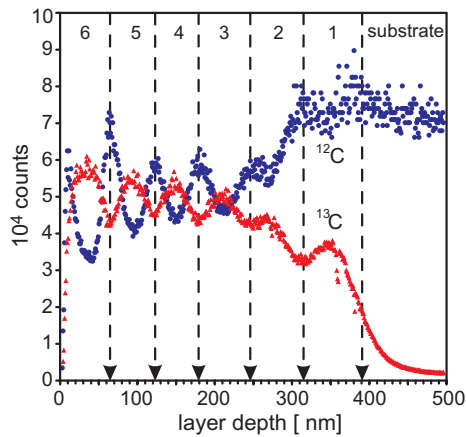


Fig. 4. SIMS depth profile of ^{12}C (dots) and ^{13}C (triangles) for the position on the graphite limiter indicated in Fig. 2. Vertical broken lines separate six individual $^{13}\text{CH}_4$ injections.

this information with the total deposited carbon amount known from colorimetry, the deposited ^{13}C amount and, hence, the deposition efficiency could be determined for each individual discharge. Table 1 summarizes the integral results of each shot series. Note that the numbers given there for the ^{13}C deposition efficiency as well as for the fraction of ^{13}C are averaged values, which vary in a quite broad range for different discharges in the series (Fig. 5). The integral value of ^{13}C deposition efficiency for graphite of 0.17% is in good agreement with the previous experiment in the roof-like geometry [2].

Reflectometry shows that an unusually high amount of carbon was deposited on tungsten in the first discharge (Fig. 3(a)). With a fraction of 94%, ^{12}C obviously dominates the deposition in this shot. Note that the deposition in this discharge was still localized near the aperture and therefore triggered by the $^{13}\text{CH}_4$ injection. Local spectroscopic observation in the light of CII and CIII lines shows that the concentration of carbon increased by a factor ≈ 2 in front of the limiter for this particular shot, whereas there was only a marginal increase in the main plasma. It indicates that the limiter itself

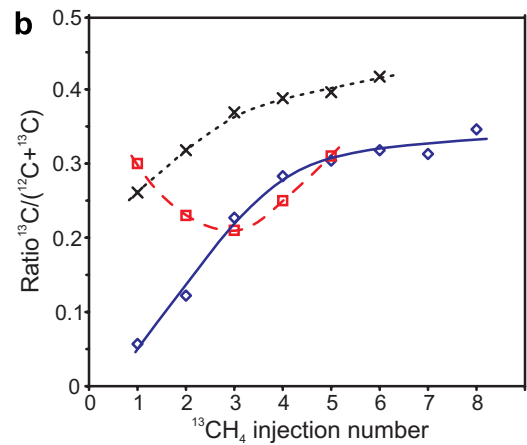
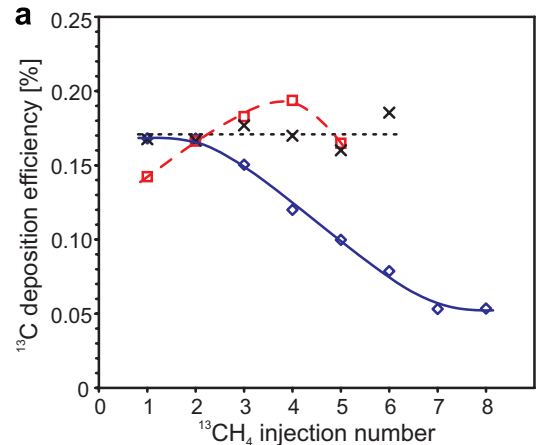


Fig. 5. Discharge resolved (a) ^{13}C deposition efficiency and (b) ^{13}C fraction for tungsten (diamonds), molybdenum (boxes) and graphite (crosses) with curves to guide the eye.

served as a carbon source before it was gradually cleaned by plasma. This explains the general tendency for the tungsten as well as the graphite limiter to exhibit an increasing ^{13}C fraction in the sequence of discharges (Fig. 5(b)).

A correlation of the ^{13}C deposition efficiency with the amount of co-deposited ^{12}C was observed (Fig. 6). This behaviour confirms findings of recent modelling studies made by the ERO code where the

Table 1

Summary of the $^{13}\text{CH}_4$ injection experiments with the numbers integrated over the discharge series

Experiment	Number of discharges in series	Injected $^{13}\text{CH}_4$ amount (molecules)	Deposited ^{13}C amount (atoms)	Deposited ^{12}C amount (atoms)	$^{13}\text{C}/(^{12}\text{C} + ^{13}\text{C})$ in the layer	^{13}C deposition efficiency
Tungsten	8	6.3×10^{20}	7.0×10^{17}	4.1×10^{18}	0.15	0.11%
Molybdenum	5	3.8×10^{20}	6.5×10^{17}	1.9×10^{18}	0.25	0.17%
Graphite	6	4.1×10^{20}	7.0×10^{17}	1.3×10^{18}	0.35	0.17%

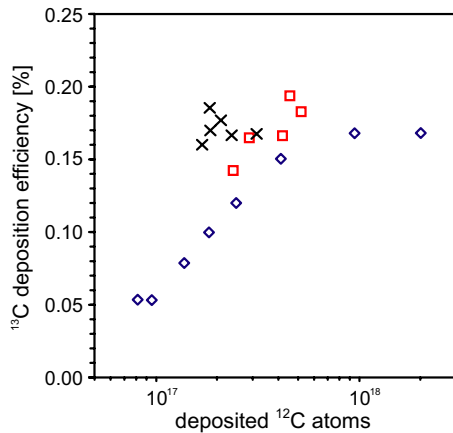


Fig. 6. ¹³C deposition efficiency as a function of co-deposited ¹²C (logarithmic scaling) for tungsten (diamonds), molybdenum (boxes) and graphite (crosses).

increasing concentration of carbon in the background flux results in higher ¹³C deposition efficiency [7]. It seems that the incoming ¹²C atoms protect the ¹³C from erosion. The comparison of the ¹³C deposition efficiencies for the different materials can be adjusted for the same value of ¹²C background deposition (Fig. 6). *E.g.* for $\approx(2-3) \times 10^{17}$ ¹²C/shot we obtain ¹³C deposition efficiencies of 0.11% for tungsten, 0.14% for molybdenum and 0.17% for graphite.

3. Summary and discussion

¹³CH₄ injection experiments were performed for tungsten, molybdenum and graphite limiters of a roof-like geometry exposed in SOL of TEXTOR. Amounts of deposited ¹²C and ¹³C were determined for each shot in the series. The ¹³C fraction of total deposited carbon tends to increase with progressing

discharge series, because the limiters were cleaned from carbon impurities by the plasma during their exposure. Some particular shots had an exceptionally low ¹³C fraction in the layer, although the deposition was still triggered by the ¹³CH₄ injection. It indicates the influence of the gas injection on the local plasma parameters leading to increased net-deposition near the injection aperture.

The ¹³C deposition efficiency shows a clear dependence on the amount of co-deposited ¹²C. This observation confirms the ERO code prediction of the protective role of ¹²C. For the same amount of deposited ¹²C, the ¹³C deposition efficiency shows a trend to lower values for materials with higher atomic mass. Similar observation was made for the injection-independent ¹²C background deposition. This dependence on the atomic mass of substrate is in qualitative agreement with the findings from the spherically-shaped limiter experiments. The material dependence is more pronounced in the spherical geometry, probably because of the shallow angle of incidence resulting in a dilution of the background flux responsible for erosion.

References

- [1] G. Federici, C.H. Skinner, J.N. Brooks, et al., Nucl. Fusion 41 (2001) 1967.
- [2] P. Wienhold, H.G. Esser, D. Hildebrandt, et al., J. Nucl. Mater. 290–293 (2001) 362.
- [3] A. Kreter, D. Borodin, S. Brezinsek, et al., Plasma Phys. Control. Fus. 48 (2006) 1401.
- [4] A. Litnovsky, P. Wienhold, V. Philipps, et al., J. Nucl. Mater., these Proceedings, doi:10.1016/j.jnucmat.2007.01.281.
- [5] U. Samm, Fusion Sci. Technol. 47 (2005) 73.
- [6] S. Brezinsek, G. Sergienko, A. Pospieszczyk, et al., Plasma Phys. Control. Fus. 47 (2005) 615.
- [7] A. Kirschner, private communication.